Journal of The Electrochemical Society, **151** (6) G377-G379 (2004)
0013-4651/2004/151(6)/G377/3/$7.00 © The Electrochemical Society, Inc.

Device Level Characterization for Energy Bandgap of Strain-relaxed SiGe and Oxide/SiGe Barrier Height

C. H. Huang,[a] D. S. Yu,[a] Albert Chin,[a,z] W. J. Chen,[b] and S. P. McAlister[c]

[a]*Department of Electronics Engineering, National Chiao Tung University Hsinchu, Taiwan, Republic of China*
[b]*Department of Mechanical Materials Engineering, National Yun-Lin Polytechnic Institute, Huwei, Taiwan, Republic of China*
[c]*Institute for Microstructural Sciences, National Research Council, Ottawa, Canada*

From the interface state density with energy plot measured by capacitance-voltage characteristics, we have derived the energy bandgap of strain-relaxed $Si_{1-x}Ge_x$ (x: 0.4 and 0.7) for the first time at the device level, because the allowed states increases sharply near the conduction and valence bandedges. We find that the energy bandgap of SiGe is reduced from 0.90 to 0.83 eV as the Ge composition increases from $Si_{0.6}Ge_{0.4}$ to $Si_{0.3}Ge_{0.7}$. In contrast, similar oxide/$Si_{1-x}Ge_x$ conduction-band barrier heights of ~3.1 eV have been obtained for both SiGe cases using Fowler-Nordheim tunneling. These results are in good agreement with published theoretical and experimental data from material level characterization. The device level characterization is especially important because the SiGe composition and material property may be altered after thermal cycles for device fabrication.
 [DOI: 10.1149/1.1705663]

Manuscript submitted August 1, 2003; revised manuscript received November 17, 2003. Available electronically April 26, 2004.

The SiGe or strained Si on strain-relaxed SiGe has a high potential to be integrated into metal oxide semiconductor field effect transistors (MOSFETs),[1-6] along with high-κ gate dielectrics,[7-12] resulting in improved mobility. The higher current drive capability of an SiGe or strained Si MOSFET, compared with its Si counterpart, can effectively improve the operation speed and circuit density, and this is equivalent to scaling the device down. To achieve integration of this technology into high-κ gate dielectric or current complementary metal oxide semiconductor processes requires device level rather than material level characterization and control. This is so because Ge in SiGe may diffuse toward the ultrathin top strained Si or oxide interface during subsequent high-temperature processes[3,13] thus altering or degrading the desired device performance. In addition, the altered device parameters are also sensitive for equivalent circuit modeling and integrated circuit design. In this paper, we have investigated, at the device level, the energy bandgap of strain-relaxed SiGe and oxide/SiGe barrier height, where large improved hole mobility,[2,5,6] excellent gate oxide integrity,[3,4] low source-drain junction leakage,[2] and high-quality silicide[14] have previously been reported. In contrast with traditional energy bandgap measurements using optical methods, performed at the materials level,[15] we deduce the SiGe energy bandgap from capacitance-voltage (C-V) measurements in metal oxide semiconductor (MOS) devices for the first time. The conduction-band barrier height of strain-relaxed $Si_{0.3}Ge_{0.7}$ and $Si_{0.6}Ge_{0.4}$ has also been obtained from the MOS devices by measuring the Fowler-Nordheim (FN) tunneling current. We find that the barrier height of ~3.1 eV is almost the same as in SiO_2/Si and the strained SiGe case.

Experimental

Four-in. p-type (100) Si wafers were used in this work on the energy bandgap and barrier height study. After 300 nm field oxide isolation and native oxide cleaning, a ~20 nm strain-relaxed $Si_{0.3}Ge_{0.7}$ or $Si_{0.6}Ge_{0.4}$ was formed on the active region by solid-phase epitaxy[13] using 900°C rapid thermal annealing. The composition of the SiGe was determined by X-ray diffraction (XRD), and good crystalline quality was confirmed by cross-sectional transmission electron microscopy (TEM) and XRD measurements.[13] A 5.0 nm thick gate oxide was then grown in dry O_2 at 850°C, for both the $Si_{0.3}Ge_{0.7}$ and $Si_{0.6}Ge_{0.4}$ samples. The gate electrode was formed after deposition of 300 nm poly-Si, phosphorus doping, and subsequent processing. More detailed SiGe material and MOSFET characterizations can be found elsewhere.[2-6,13,14] The energy bandgap of the unstrained SiGe layer can be obtained from C-V measurements of the interface trap density. The oxide/SiGe conduction-band barrier height was determined from measurements of the FN tunneling currents in inversion conditions.

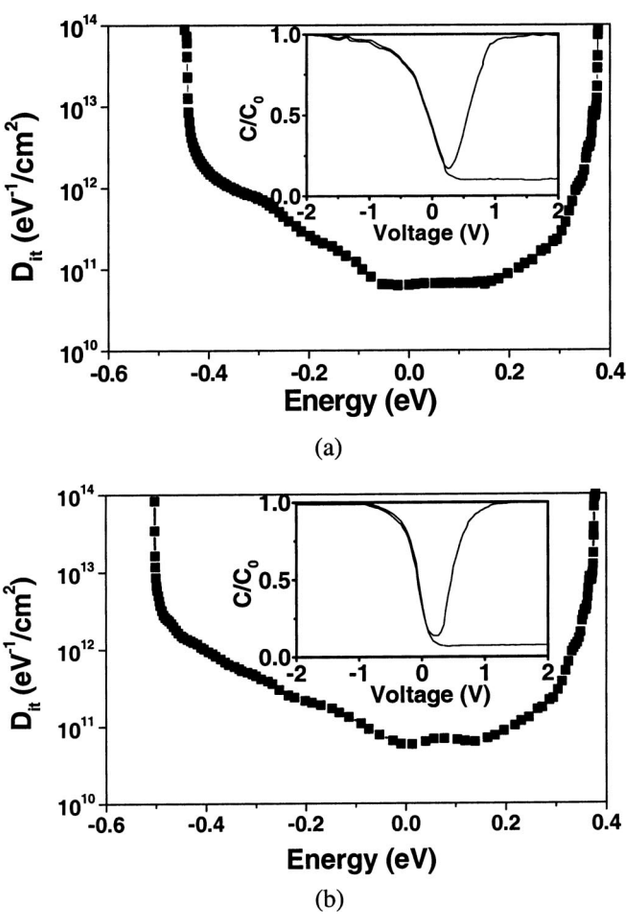

Figure 1. Interface trap density as a function of energy for 5.0 nm thermal oxides grown on (a) $Si_{0.3}Ge_{0.7}$ and (b) $Si_{0.6}Ge_{0.4}$. The data was obtained from the quasi-static and high-frequency C-V measurements of MOS devices, shown in the insets.

[z] E-mail: achin@cc.nctu.edu.tw

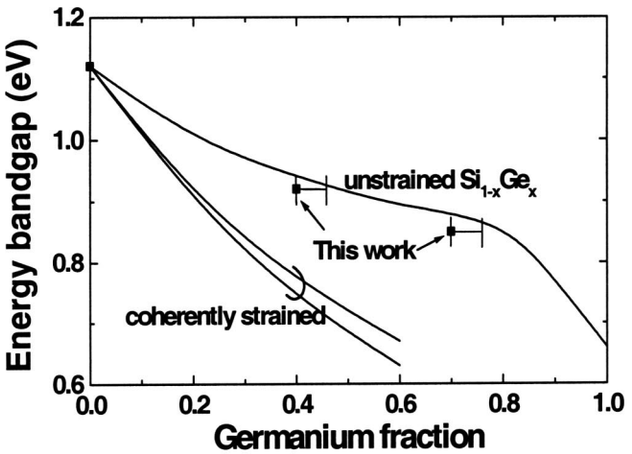

(a)

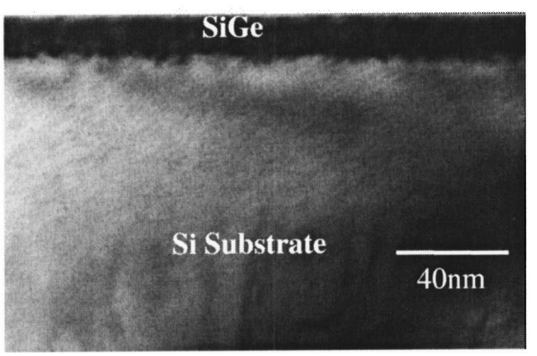

(b)

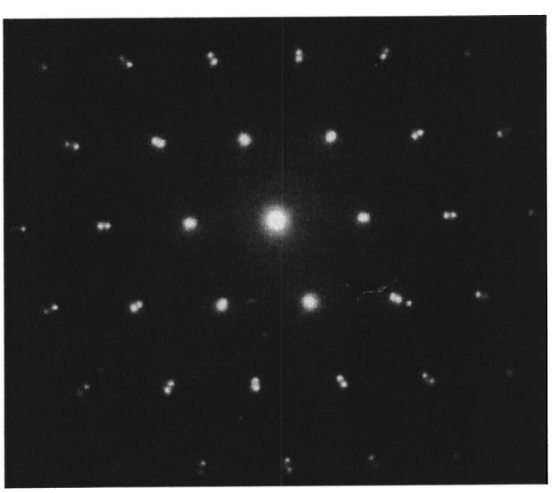

(c)

Figure 2. (a) The energy bandgap as a function of Ge mole fraction, (b) cross-sectional TEM of solid-phase epitaxy formed SiGe/Si, and (c) the electron diffraction pattern. The error bar in the Ge composition is due to the slightly higher Ge composition at the oxide/SiGe interface of the MOSFETs and was obtained from secondary-ion mass spectrometry analysis (Ref. 15). The bulk Ge composition was determined by XRD. Good uniformity and homogeneity are evidenced from the cross-sectional TEM image and the electron diffraction pattern.

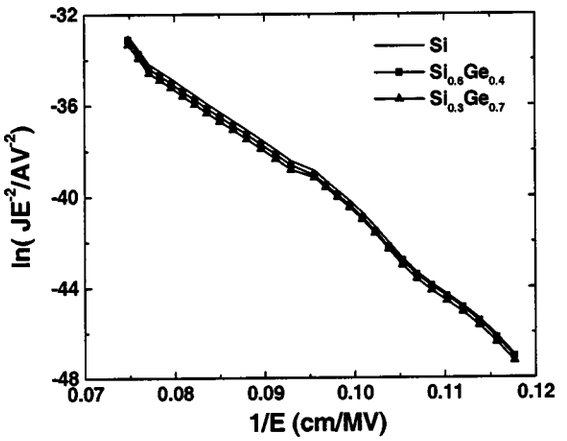

Figure 3. Comparison of tunneling current data obtained for MOSFETs with different Ge compositions, plotted as J/E^2 *vs.* $1/E$.

Results and Discussion

Figures 1a and b show the interface trap density with energy for $Si_{0.3}Ge_{0.7}$ and $Si_{0.6}Ge_{0.4}$, respectively. The interface trap density was derived from the low- and high-frequency C-V measurements (see insets). The low minimum interface trap density of $\sim 6 \times 10^{10}$ eV^{-1}

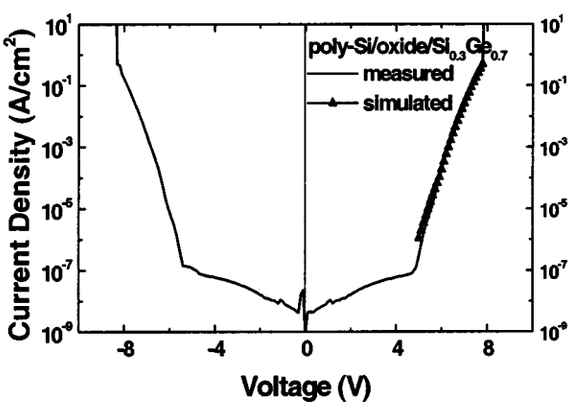

(a)

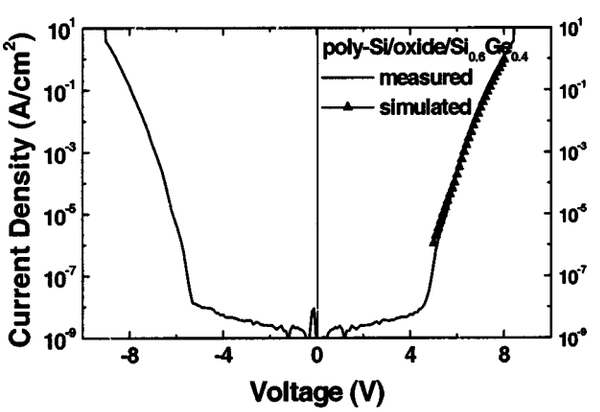

(b)

Figure 4. The voltage dependence of the absolute value of the measured and simulated FN tunneling gate current density for MOSFETs with different Ge compositions: (a) $Si_{0.3}Ge_{0.7}$ and (b) $Si_{0.6}Ge_{0.4}$.

cm^{-2} and small oxide charge density (less than -1×10^{11} cm^{-2}), obtained for both SiGe samples, indicate good interface and oxide properties. The interface state density increases rapidly with energy near the conduction and valence bandedges, because of the large number of allowed states there. This permits direct determination of the bandgap from the energy difference between the conduction and valence bandedges. We obtained bandgaps of 0.83 eV ($Si_{0.3}Ge_{0.7}$) and 0.90 eV ($Si_{0.6}Ge_{0.4}$), from the interface trap density data. To our knowledge, this is the first report of energy bandgap obtained directly from MOS devices using an electrical method.

In Fig. 2a we show the Ge composition dependence of the bandgap energy. We have also added the cross-sectional TEM image and electron diffraction pattern of solid-phase epitaxy formed SiGe/Si in Fig. 2b and c, respectively. The uniform thickness of the SiGe layer from TEM (Fig. 2b) and the good homogeneity from clearly separated Si and SiGe lattice points from electron diffraction (Fig. 2c) are important for device fabrication and parameter extraction. The measured bandgap data is close to the theoretical values for strain-relaxed SiGe.[16] An advantage of our approach is that it is performed at the device level, so that any strain and composition changes in the SiGe during processing are automatically included.

The magnitude of the oxide/SiGe barrier height is important for SiGe MOS devices. The barrier height energy can be obtained from the FN tunneling current density given by

$$J_{FN} = AE_{ox}^2 \exp[-B/E_{ox}] \quad [1]$$

where E_{ox} is the electric field in the oxide, and A and B are directly related to the barrier height and the effective mass in the oxide. In Fig. 3 we compare the inversion FN tunneling current for $Si_{0.7}Ge_{0.3}$, $Si_{0.4}Ge_{0.6}$, and Si, as a J/E_{ox}^2 *vs.* $1/E_{ox}$ plot. The nearly identical results for the three cases suggest that the barrier heights and effective masses are almost the same.

In Fig. 4a and b, we compare simulated and measured FN tunneling data for $Si_{0.3}Ge_{0.7}$ and $Si_{0.6}Ge_{0.4}$, respectively. The measured and simulated data match well using the values for the effective mass and barrier height in Table I. It is significant that the barrier height between strain-relaxed SiGe and the oxide conduction-band is almost the same as that between Si and its oxide.

Note that good accuracy is required for both energy bandgap and barrier height extraction. The voltage accuracies of HP4284 for C-V measurements and HP4155B for I-V measurements are 5 mV and 1 mV with typical errors of $\pm 3\%$, respectively. Therefore, the typical error for energy bandgap extraction from C-V is 5 meV. The error for conduction-band barrier height is less than 1 meV because the barrier height is in the exponential term of Eq. 1, and the calculated current must fit the measured data in a wide range of voltage points shown in Fig. 4. This result is consistent with the value obtained from unstrained poly-$Si_{0.3}Ge_{0.7}$ and oxide.[17] The valence-band barrier height increase with increasing Ge composition reduces hole injection into the oxide and oxide traps, which can improve the device reliability.

Table I. The energy bandgap, conduction-band barrier height, and effective mass of strain-relaxed SiGe layers.

	E_g (eV)	Φ_B (eV)	m_{ox}^*/m_0
$Si_{0.3}Ge_{0.7}$/oxide	0.83	3.08	0.50
$Si_{0.6}Ge_{0.4}$/oxide	0.90	3.10	0.50
Si/oxide	1.12	3.10	0.50

Conclusion

We have studied the SiGe energy bandgaps and oxide barrier heights of unstrained $Si_{0.3}Ge_{0.7}$ and $Si_{0.6}Ge_{0.4}$ using C-V measurements and FN tunneling currents, respectively. The energy bandgap of SiGe is reduced from 0.90 to 0.83 eV as the Ge composition increases from $Si_{0.6}Ge_{0.4}$ to $Si_{0.3}Ge_{0.7}$. The conduction-band barrier height for both SiGe/oxide cases remains the same as that for SiO_2/Si.

Acknowledgment

The work was supported by NSC (91-2215-E-009-038) of Taiwan, Republic of China.

National Chiao Tung University assisted in meeting the publication costs of this article.

References

1. T. Mizuno, N. Sugiyama, H. Satake, and S. Takagi, *Technical Digest for Symposium on VLSI Technology*, p. 210 (2000).
2. Y. H. Wu and A. Chin, *IEEE Electron Device Lett.*, **21**, 350 (2000).
3. Y. H. Wu, A. Chin, and W. J. Chen, *IEEE Electron Device Lett.*, **21**, 289 (2000).
4. Y. H. Wu, A. Chin, and W. J. Chen, *IEEE Electron Device Lett.*, **21**, 113 (2000).
5. C. H. Huang, S. B. Chen, and A. Chin, *IEEE Electron Device Lett.*, **23**, 710 (2002).
6. C. H. Huang, M. Y. Yang, A. Chin, W. J. Chen, C. X. Zhu, B. J. Cho, M.-F. Li, and D. L. Kwong, *Technical Digest for Symposium on VLSI Technology*, p. 119 (2003).
7. Y. T. Hou, M. F. Li, H. Y. Yu, Y. Jin, and D. L. Kwong, *Tech. Dig. - Int. Electron Devices Meet.*, **2002**, 731.
8. L. Kang, Y. Jeon, K. Onishi, B. H. Lee, W. J. Qi, R. Nieh, S. Gopalan, and J. C. Lee, *Technical Digest for Symposium on VLSI Technology*, p. 44 (2000).
9. T. Nagi, W. J. Qi, X. Chen, R. Sharma, J. L. Fretwell, J. C. Lee, and S. K. Banerjee, *Technical Digest for 58th Device Research Conference*, p. 21 (2000).
10. X. Guo, X. Wang, Z. Luo, T. P. Ma, and T. Tamagawa, *Tech. Dig. - Int. Electron Devices Meet.*, **1999**, 137.
11. A. Chin, C. C. Liao, C. H. Lu, W. J. Chen, and C. Tsai, *Technical Digest for Symposium on VLSI Technology*, p. 135 (1999).
12. A. Chin, Y. H. Wu, S. B. Chen, C. C. Liao, and W. J. Chen, *Technical Digest for Symposium on VLSI Technology*, p. 16 (2000).
13. Y. H. Wu, W. J. Chen, A. Chin, and C. Tsai, *Appl. Phys. Lett.*, **74**, 528 (1999).
14. C. Y. Lin, W. J. Chen, C. H. Lai, A. Chin, and J. Liu, *IEEE Electron Device Lett.*, **23**, 464 (2000).
15. R. Braunstein, A. R. Moore, and F. Herman, *Phys. Rev.*, **109**, 695 (1958).
16. R. People, *Phys. Rev. B*, **32**, 1405 (1985).
17. V. E. Houtsma, J. Holleman, C. Salm, F. P. Widdershoven, and P. H. Woerlee, *IEEE Electron Device Lett.*, **20**, 314 (1999).